

# Effect of the Flow Curve Determination on the Thinning of Drawn Parts

MARTIN LÁSZLÓ KÖLÜS<sup>1</sup>, RICHÁRD BORBÉLY<sup>2</sup>, DÁNIEL SZÓKE<sup>3</sup>, GÁBOR JÓZSEF BÉRES<sup>4</sup>

<sup>1</sup>John von Neumann University GAMF Faculty of Engineering and Computer Science, Department of Innovative Vehicles and Materials, Mechanical- and Laser Beam Technologies Research Group, kolus.martin@gamf.uni-neumann.hu

<sup>2</sup>John von Neumann University GAMF Faculty of Engineering and Computer Science, Department of Innovative Vehicles and Materials, Mechanical- and Laser Beam Technologies Research Group, borbely.richard@gamf.uni-neumann.hu

<sup>3</sup>John von Neumann University GAMF Faculty of Engineering and Computer Science, Department of Innovative Vehicles and Materials, Mechanical- and Laser Beam Technologies Research Group

<sup>4</sup>John von Neumann University GAMF Faculty of Engineering and Computer Science, Department of Innovative Vehicles and Materials, Mechanical- and Laser Beam Technologies Research Group, beres.gabor@gamf.uni-neumann.hu

*Abstract. This study presents the results of finite element simulations based on different variations of the flow curve of DC04 automotive thin sheet. The aim of our research is to investigate how different flow curve equations affect the variation of sheet thickness in cup drawing tests. In order to exclude other influencing factors in the experiment, both the sheet material and the geometric properties of the specimen, as well as the external state factors were considered to be the same in all cases. The finite element simulations were performed using Simufact 2021.1 software. Our results shows that there are no significant differences in wall thicknesses until we reach the zone of double necking, where essential differences are observed.*

*Keywords: Flow curve, Thinning, Cup drawing test, DC04 sheet metal*

## Introduction

Nowadays the importance of sheet metals in the industry is increasing. Many sheet forming technologies are investigated numerically with one very important input parameter being the flow curve. The most common method for flow curve definition is the tensile test [1], which is not reliable for high strains due to the necking phenomenon. For this reason, we used compression test as well, that resulted two-or-three magnitude higher strains than in case of tension test [2]. Although compression tests on thin sheet metals may seem extremely unusual with the aim of flow curve definition, its potential is already recognized and researched by Kraus et al. [3], and Coppieters et al. [4,5].

After evaluating our results from the tensile test and the compression test, we plotted them on the same graph. Then we fitted the Hockett-Sherby flow curve equation [6] to our points. We were able to do this by using non-linear regression method [7]. This resulted two different flow curve equations. In the first

case, only the values obtained from the tensile test data, yet in the second case, the values obtained from the curve fitted to the full set of points (tensile test + compression test) were used as input parameters for the simulation.

In the following, we will discuss the methods of recording the flow curve, the necessary input parameters for the simulation, how to obtain them and what we have experienced in the final results of the simulations.

## 1. Methods and materials used for research

### 1.1. Material

The material used for the experiments is the grade of DC04 sheet metal. This is a commercial, cold-rolled mild steel with a ferritic structure in fact, and with very good ductility properties thanks to it [8].

### 1.2. The tensile test

The tensile tests were carried out according to ISO 6892-1:2019 standard. The specimens were also specified based on the description of the mention standard. The quasi-static experiments were carried out on an Instron 4482 universal testing machine, next to a constant motion speed of 10 mm/min, at room temperature, with three times repeating rate. The elongation of the specimens was monitored by means of an Instron AVE video extensometer, while the load on the specimens were measured by means of a load cell mounted on the cross slide of the machine. Figure 1. shows a specimen clamped into the frame, as an example.



*Figure 1. One clamped specimen during the tension test*

### 1.3. The uniaxial compression test

The compression test was done on ZD40 universal testing machine, which is shown in Figure. 2. The reason why we chose this device is that it can provide a significant load that is enough to reach much higher strains. For the test, four different loads were used in the following manner: 120; 160; 200; 240 [kN]. The cross slide motion speed was approximately 3-5 mm/min during the test.



Figure 2. The ZD40 universal testing machine

The compression tests were carried out at room temperature, too. In order to reach the lowest amount of friction, BWS lubricating oil was applied to the surfaces of the test pieces in contact with the tools, and a thin polytetrafluoroethylene foil ( $\sim 0,1$  mm) was also placed between the two surfaces.

Of paramount importance for the experiment was to ensure the best possible lubrication conditions, thus reducing the uncertainty caused by friction. To this end, we have chosen this lubrication form and lubricants with excellent friction reducing properties.

For the test we used cylindrical specimens with initial diameter of  $10\pm 0.1$  mm and with 1 mm nominal thickness. The accurate thickness was measured with a mechanical micro-meter before each compression. As it is expected, significant corrections had to be carried out during the flow curve calculations, due to the exceedingly small ratio of height to diameter. In Figure 3, a specimen after the compression test is shown.

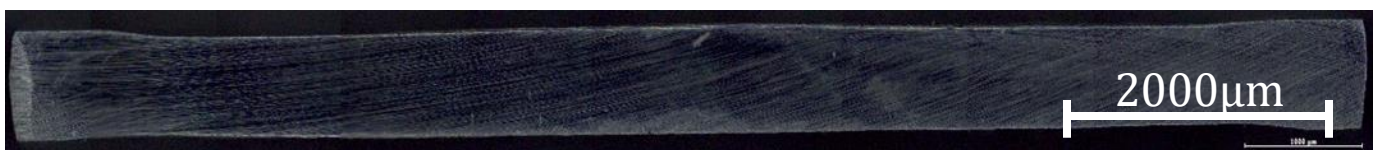


Figure 3. Specimen cross-section after compression test

## 2. Obtaining the flow curve

### 2.1. Results from tensile test

As we mentioned earlier, standard tension tests were carried out to measure the load and the longitudinal strain. Then these values were used to calculate the true specimen stress and the true strain. The results were plotted on diagrams, of which a characteristic curve is shown Figure 4.

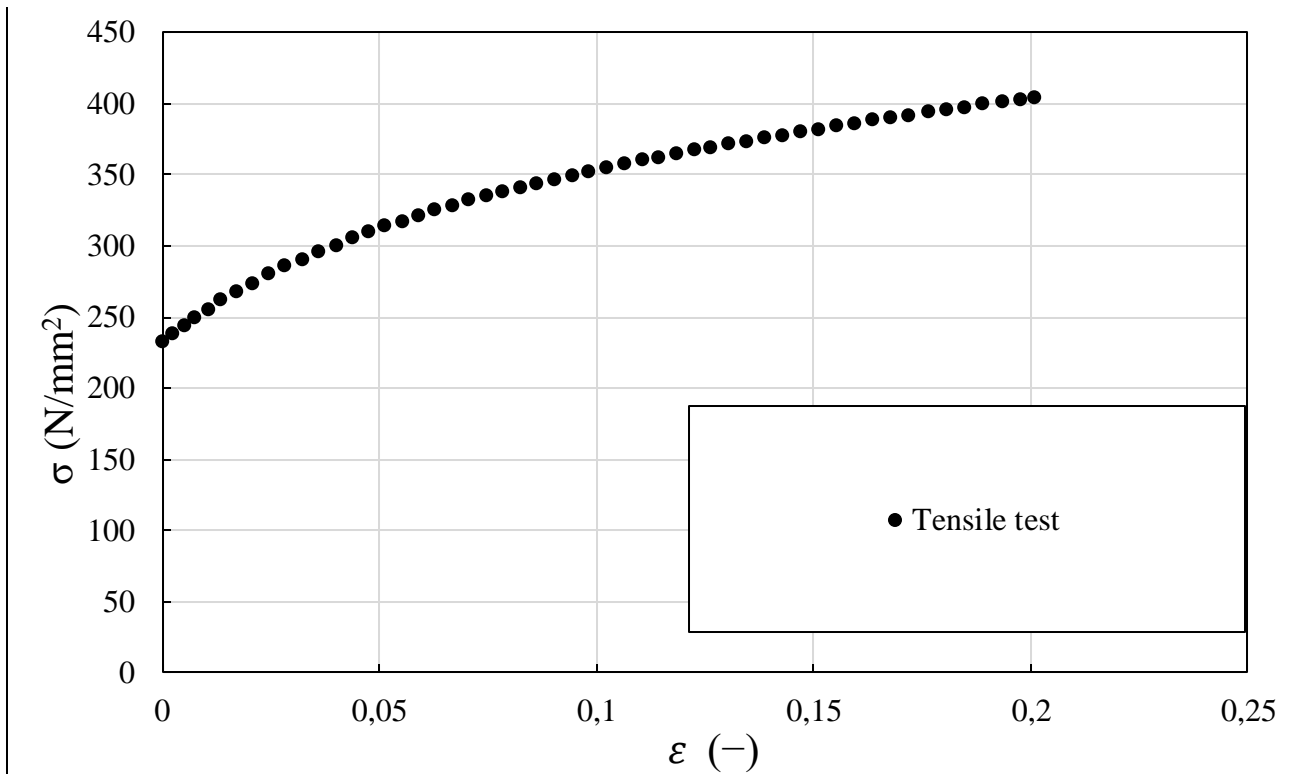


Figure 4. The results of the tensile test

It can be observed that the results obtained from tensile tests cover the deformation range up to 0.2 true strain.

### 2.2. Results from compression test

The deformation and flow strength were determined before the flow curve was constructed. The strain was determined using the following relationship [2]:

$$\bar{\varepsilon} = \ln \frac{h_0}{h_1} = \ln \left( \frac{h_0}{h_0 - \Delta h} \right) \quad (1)$$

The flow stress was derived based on the proposals of Christiansen et al [9].

$$\bar{P} = 2\sigma_0 \left( \frac{h_0 - \Delta h}{\mu(D_0 + \Delta D)} \right)^2 \left[ \exp \left( \frac{\mu(D_0 + \Delta D)}{h_0 - \Delta h} \right) - \frac{\mu(D_0 + \Delta D)}{h_0 - \Delta h} - 1 \right] \quad (2)$$

where  $\bar{P}$  is the surface pressure,  $\sigma_0$  is the yield strength,  $h_0$  is the initial height and  $D_0$  is the initial diameter. The results were plotted alongside the tensile test data (Figure 5.)

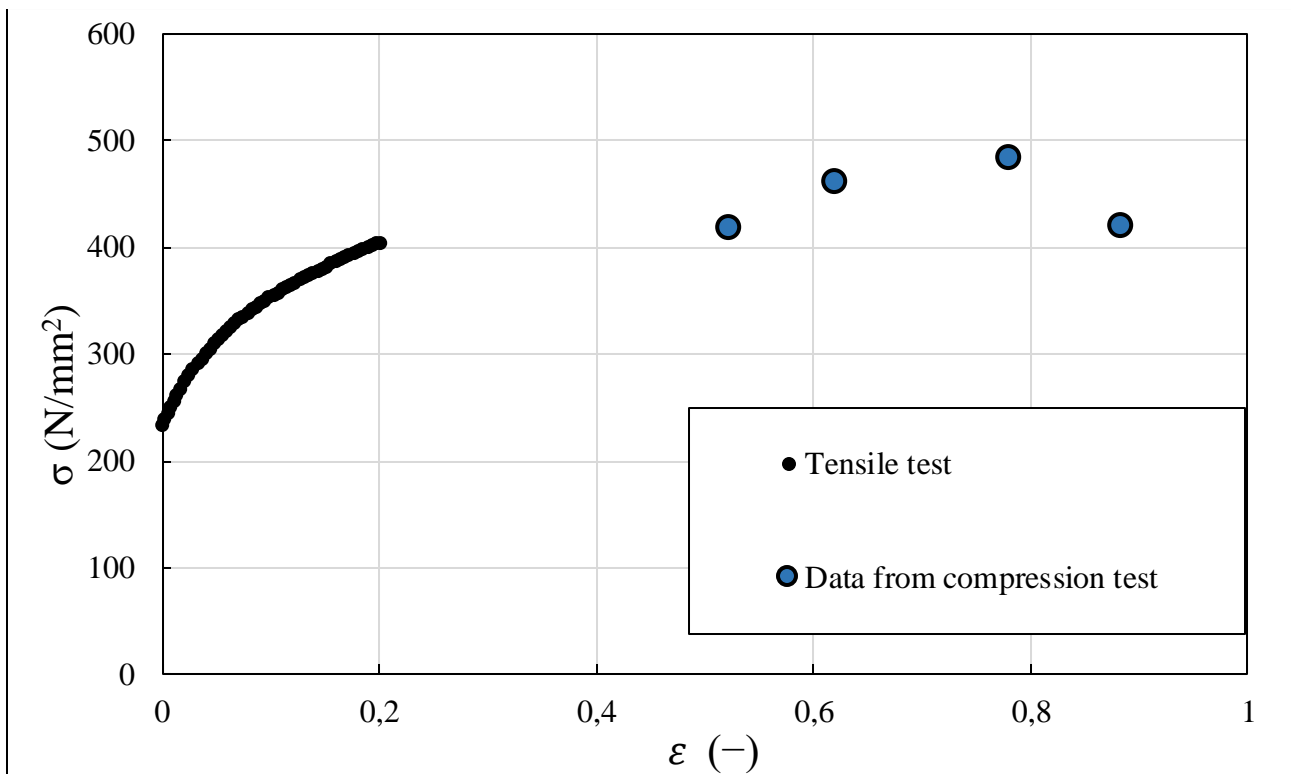


Figure 5. The jointed results of the tension and the compression tests

Complementing our tensile test results, we have created a point set that gives a picture of the deformation range up to 0.9 true strain.

### 2.3. Determining the flow curve

As mentioned before, an accurate knowledge of the flow curve for the material is a prerequisite for running finite element simulations. The Hockett-Sherby equation [6]:

$$\sigma = \sigma_s - \exp(-(N\epsilon)^p) (\sigma_s - \sigma_y) \quad (3)$$

was used in the simulation environment, which is well-known and used worldwide among other theories related to the stress strain behaviour of metallic materials. The equation includes four material parameters, such as the yield strength ( $\sigma_y$ ), the saturation stress ( $\sigma_s$ ) and the constants related to the strain evolution (N and p) [10]. In the first case, using data obtained purely from tensile testing, the flow curve equation for the DC04 sheet metal was determined. In the second case, we complemented our tensile test results with results obtained from compression test. This resulted in a flow curve covering a larger range of deformation, with an equation that differs from the flow curve obtained from the tensile test. Figure 6 shows the flow curves obtained with both tensile and compression test.

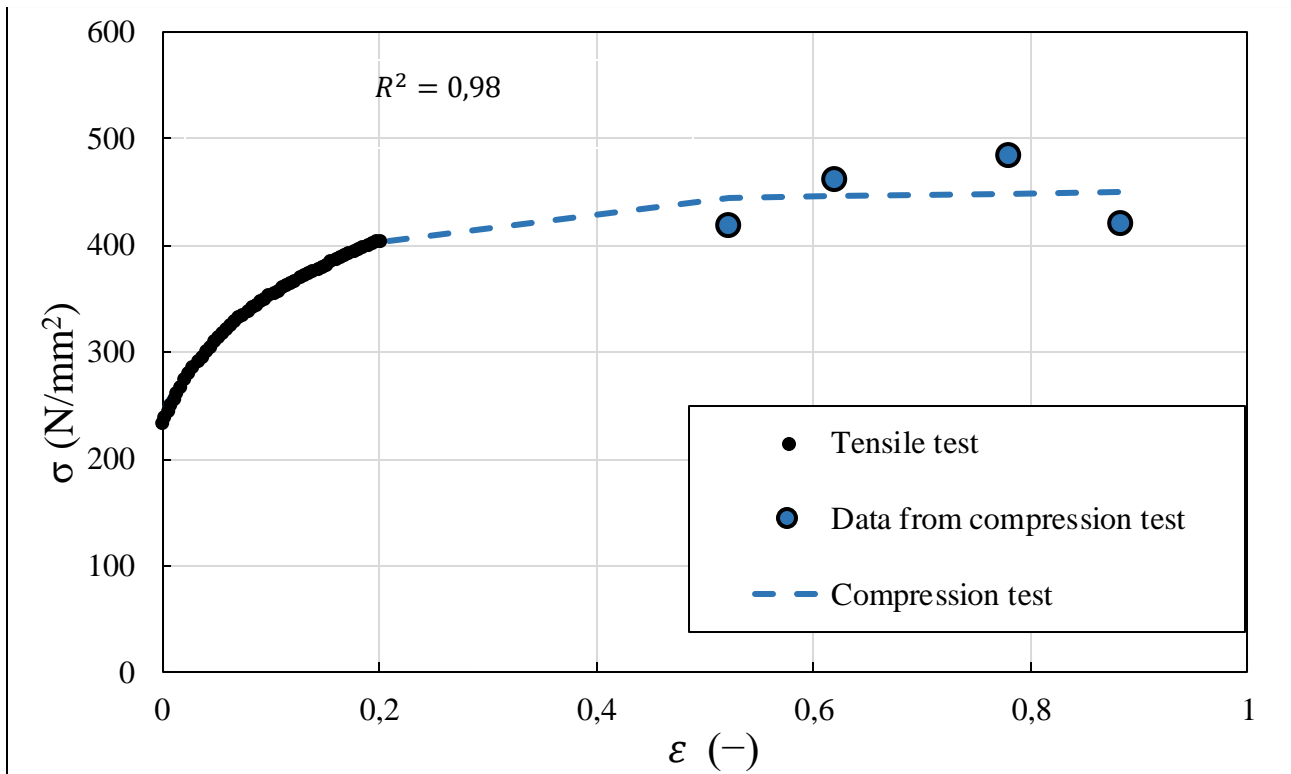


Figure 6. The extended flow curve using both tension and compression data

The curve marked with the blue dashed line is the fitted flow curve. Nonlinear regression method was used to achieve the fit.  $R^2$  shows the degree of precision between the measured and calculated results.

Table 1. shows the input parameters obtained from the flow curves.

	$\sigma_y$	$\sigma_s$	$N$	$p$	$\epsilon$
Tensile	240	456	8,60	0,89	0,20
Compression test	240	450	7,56	0,96	0,88

Table 1. The input parameters obtained from the flow curves

In Table 1.  $\sigma_y$  refers to yield strength,  $\sigma_s$  is the saturation stress,  $N$  and  $p$  are material constants and  $\epsilon$  is the strain. For the data obtained from the tensile test and the data extracted from the compression test, the difference between  $N$  and  $p$  parameters is about 10%.

### 3. The finite element simulation

In order to exclude other influencing factors in the experiment, the geometric properties of the specimen, as well as the external state factors were considered to be the same in all cases. The finite element simulations were performed using Simufact 2021.1 software. The simulation is designed to run a cup drawing test, as this test is carried out under almost identical conditions as the forming technologies used in the industry.

### 3.1. The input parameters used

In order to make the simulation as realistic as possible, it is essential that the input parameters are correctly entered. During the simulations, the element size was 1,4 mm, the element number was 6744 for a flat blank with initial Ø66 mm, and the element type was hexahedral. The Coulomb friction model was used with the value of 0.12.

The forming limit diagram (Figure 7.) is also an essential parameter, which was obtained by the literature [11]. To describe the deformation behaviour, the Hill'48 yield criterion [12] calculated from the average Lankford coefficient was applied. The validation of the simulations is in progress, however this study deals with the comparison of the numerical results only.

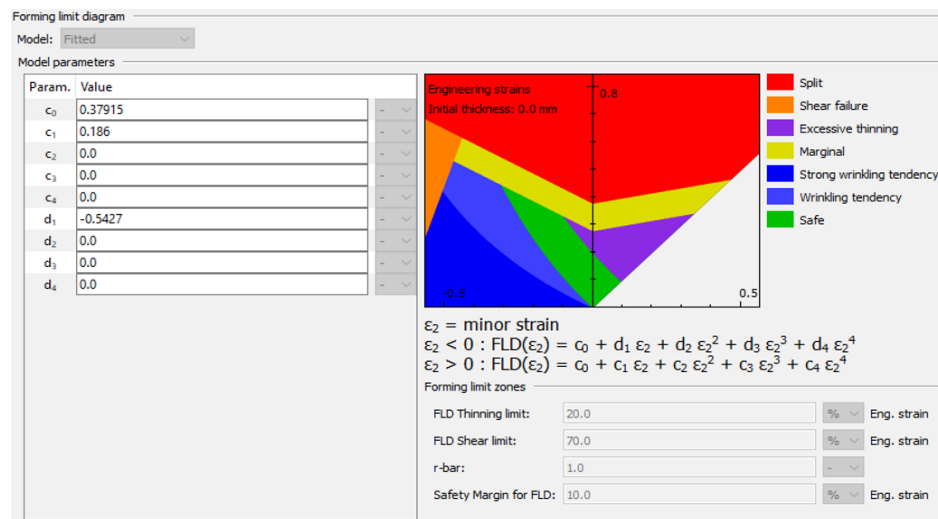


Figure 7. The forming limit diagram used during the simulations

In our case, we do not attach much importance to the forming limit diagram as we do not come close to the material failure in the simulations.

### 3.2. The results of the simulations

Figure 8. shows one representative result of the simulations as well as the thickness measurement method. The thickness was investigated in the virtual sections that lie parallel and perpendicular to the rolling direction.

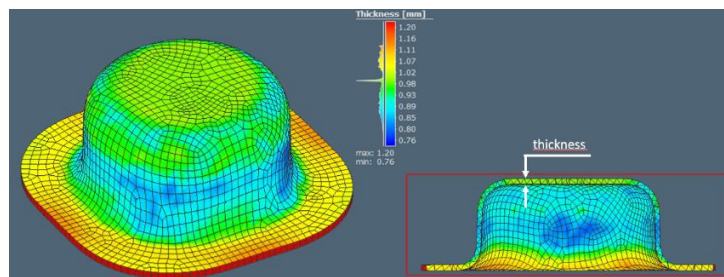


Figure 8 Result of the drawing test' simulation

Figure 8. clearly shows that the sheet thickness varies between 0,76 mm (at the punch corner) and 1,20 mm (at the flange) over the whole specimen.

After running all simulations, we plotted the change of the sheet thickness as a function of distance from the centre. We examined both the rolling direction (Figure 9.) and the transverse direction (Figure 10.), too.

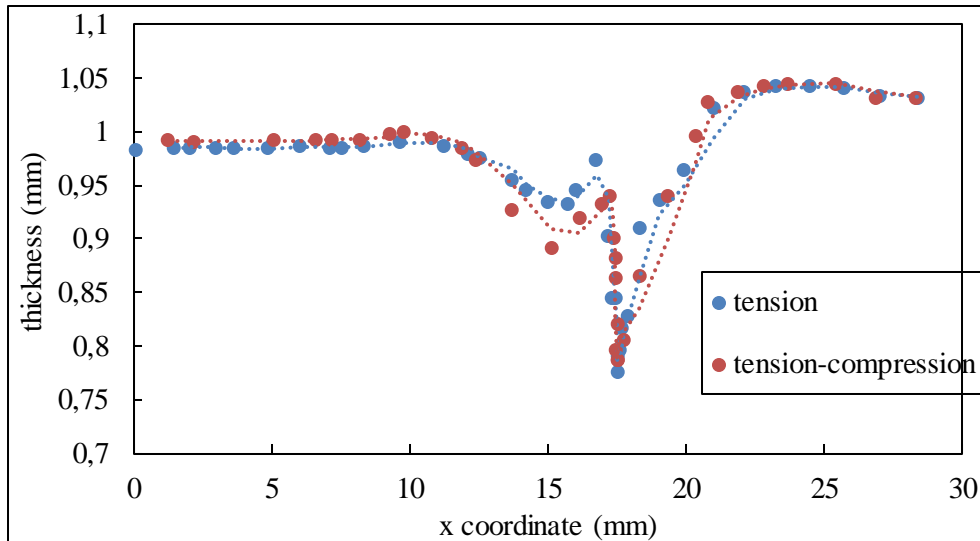


Figure 9. Change of thickness over the x coordinate (rolling direction)

Figure 9. shows that there is a good correlation between the two curves. The blue dots represents the results gained only from the tensile data, while the brown dots represents the results earned from the extended flow curve (tensile test + compression test).

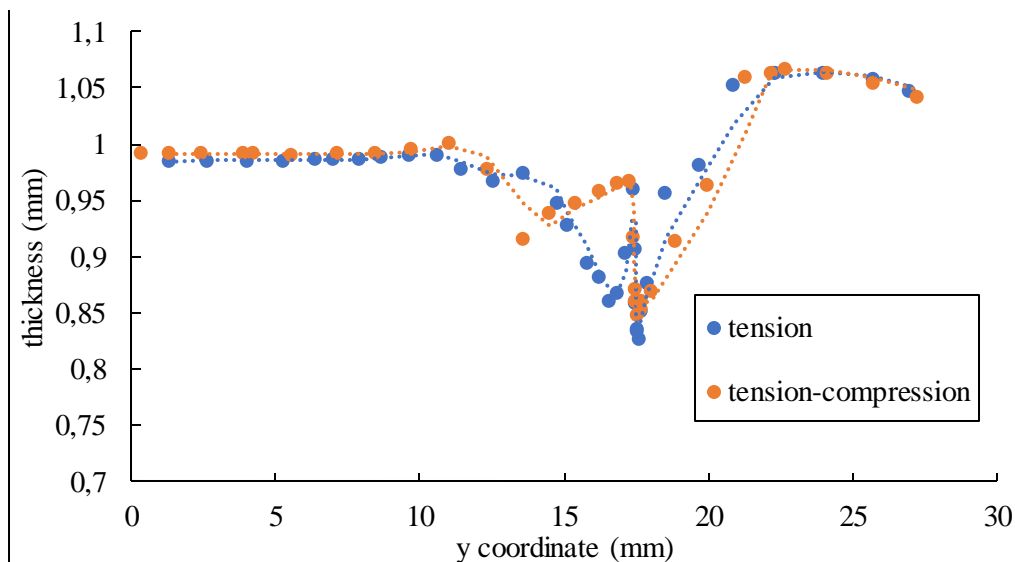


Figure 10. Change of thickness over the y coordinate (transvers direction)

However, in the case of the transvers direction, the results show that there is an essential difference between the two curves close to the necking zone. Double-necking is appeared using the pure tension-based curve, and simple neck occurred when calculating with the extended (tension + compression) flow curve data.

## Conclusion

We used experimental results of tensile and compression test to obtain the flow curve of DC04 thin sheet. Finite element simulations were made by using the different input parameters from the flow curves we determined. An essential amount of difference occurred in the zone of double necking phenomenon. Even in the case of a piece cut along the rolling direction, the deviation is about 10%, while in the transverse direction the deviation is much larger. To reduce uncertainty and verify our results, we plan to carry out further tests and finite element simulations.

## Acknowledgement

We would like to thank John von Neumann University for providing us with the tools and materials essential for this research, and we would like to thank all our colleagues who contributed in some way to the research.

## References

- [1] D. Banabic, H.-J. Bunge, K. Pöhlandt, A.E. Tekkaya, "Formability of Metallic Materials", Springer, Berlin, Heidelberg, New York, Barcelona, Hong Kong, London, Milan, Paris, Singapore, Tokyo, 2000.
- [2] Kurt Lange, Klaus Pöhlandt, Ragu S. Raghupathi, John D. Sainter, Wolfgang J. Sauer, John A. Schey, Klaus J. Wienmann, G.E.O. Widera, "Handbook of Metalforming", Society of Manufacturing Engineers, Dearborn, Michigan 48121, U.S.A, 1985.
- [3] Kraus, M., Lenzen, M., Merklein, M., "Contact pressure-dependent friction characterization by using a single sheet metal compression test", *Wear*, 476, 203679, 2021, <https://doi.org/10.1016/j.wear.2021.203679>.
- [4] Coppieters, S., Traphöner, H., Stiebert, F., Balan, T., Kuwabara, T., Tekkaya, A.E., "Large strain flow curve identification for sheet metal", *Journal of Materials Processing Tech.*, 308, 117725, 2022, <https://doi.org/10.1016/j.jmatprotec.2022.117725>.
- [5] Coppieters, S., Jackel, M., Kraus, C., Kuwabara, T., Barlat, F., "Influence of a Hydrostatic Pressure Shift on the Flow Stress in Sheet Metal", *Procedia Manufacturing*, 47, 1245-1249, 2020, <https://doi.org/10.1016/j.promfg.2020.04.196>.
- [6] Hockett, J.E., Sherby, O.D., *J. Mech. Phys. Solids*, 23, 87-98, 1975.
- [7] Jekel, C.F., Venter, G., Venter, M.P. et al., *Int J Mater Form*, 12: 355, 2019, <https://doi.org/10.1007/s12289-018-1421-8>.
- [8] Thyssenkrupp Steel Europe AG: Product Information, Deep-drawing steels DD, DC and DX. 2018 version 0
- [9] P. Christiansen, P.A.F. Martins, N.Bay, "Friction Compensation in the Upsetting of Cylindrical Test Specimens", *Experimental Mechanics*, 56:1271-1279, 2016.

- [10] Xin-cun Zhuang et al., Determination of Flow Curve and Plastic Anisotropy of Medium-thick Metal Plate: Experiments and Inverse Analysis, Journal of Iron and Steel Research, International, 2015.
- [11] Paul, S.K., "Theoretical analysis of strain- and stress-based forming limit diagrams" J Strain Analysis 48(3), 177-188, 2013.
- [12] Hill, R., "A theory of the yielding and plastic flow of anisotropic metals. The hydrodynamics of non-Newtonian fluids. I", 281-297, 1947.



© 2023 by the authors. Creative Commons Attribution (CC BY) license (<http://creativecommons.org/licenses/by/4.0/>).